New Journal of Physics
An Institute of Physics and Deutsche Physikalische Gesellschaft Journal

Coloured phase singularities

M V Berry
H H Wills Physics Laboratory, Tyndall Avenue, Bristol BS8 1TL, UK
URL: http://www.phy.bris.ac.uk/staff/berry_mv.html

New Journal of Physics **4** (2002) 66.1–66.14 (http://www.njp.org/)
Received 11 July 2002, in final form 2 August 2002
Published 5 September 2002

Abstract. For illumination with white light, the spectra near a typical isolated phase singularity (nodal point of the component wavelengths) can be described by a universal function of position, up to linear distortion and a weak dependence on the spectrum of the source. The appearance of the singularity when viewed by a human observer is predicted by transforming the spectrum to trichromatic variables and chromaticity coordinates, and then rendering the colours, scaled to constant luminosity, on a computer monitor. The pattern far from the singularity is a white that depends on the source temperature, and the centre of the pattern is flanked by intensely coloured 'eyes', one orange and one blue, separated by red, and one of the eyes is surrounded by a bright white circle. Only a small range of possible colours appears near the singularity; in particular, there is no green.

1. Introduction

Fundamental to diffraction optics is the fact that the spectrum of a source is changed by propagation: for example the field of a white-light source that has passed through a diffraction grating is differently coloured in different places. A recent insight (Gbur *et al* 2002a, 2002b, Foley and Wolf 2002, Ponomarenko and Wolf 2002) is that these spectral changes are most rapid and extreme near phase singularities (alternatively called intensity zeros, wave dislocations, topological charges, or optical vortices (Nye 1999, Soskin and Vasnetsov 2001)) of the spectral component fields in the relevant spectral range. These theoretically predicted phenomena, associated with complete destructive interference, have been observed (Popescu and Dogariu 2002).

My purpose here is to describe how such spectral changes would appear to the human eye as a characteristic pattern of colours near a typical isolated phase singularity generated by a white-light source, when the light in this dark region of the image is scaled to constant luminosity.

1367-2630/02/000066+14$30.00

This involves translating the spectra into standard colour coordinates, and then rendering them as simulations on a screen or in print. The local colour pattern has an unexpectedly rich structure, and is universal, that is independent of details, up to trivial linear coordinate rescaling and a straightforward dependence on the colour temperature of the source.

Since zeros of light waves are the singularities of wave optics, this study can be regarded as a companion to Berry and Klein (1996) (see also Berry and Wilson 1994), describing universal diffraction colours near the singularities of ray optics, namely caustics. In the present study, as in the previous one, rendering the interference colours from the rather simple physics is not a trivial matter, exemplifying the fact that although it is often convenient to use colours on a computer monitor, or on the printed page, to represent data (e.g. to distinguish several different curves on a graph), or as decoration, it is less easy to use colour to represent colour.

The local spectral expansion near a zero is described in section 2. This is converted into colour coordinates in section 3, and rendered in section 4. The main results of this paper are the simulations, shown in figure 7; readers uninterested in the theoretical basis of the simulations should proceed directly to these illustrations. A proposed experimental procedure to observe the predicted colour phenomena is outlined in section 5.

2. Diffraction spectrum near the singularity

Phase singularities have codimension 2 and so typical local phenomena associated with them can be studied in the plane, denoted $\boldsymbol{r} = \{x, y\}$. The white light source will be regarded as a temporally incoherent mixture of wavenumbers k with spectrum $S_0(k)$. Examples are the flat spectrum $S_0 = 1$, and black-body radiation with a given temperature, for which S_0 is a Planck spectrum. The optical field after propagation from this source will be considered as temporally incoherent but spatially coherent.

Consider now any diffraction process that produces an isolated zero of the component fields k, at which the light, represented by a complex scalar field $\psi(\boldsymbol{r}; k)$, has a simple zero; in general, the zero for each k will be in a different place (so the total light intensity never vanishes). Here the term 'isolated' will be used in the technical sense that the k dependence of the position of the zero is assumed to be linear over the visible range, and the position dependence of ψ is linear over the spatial range considered.

It is convenient to choose the origin of coordinates to lie at the zero for yellow light (wavelength $\lambda = \lambda_Y = 560$ nm), and define the wavenumber by

$$k = \frac{\lambda_Y}{\lambda} \tag{1}$$

(i.e. $k_Y = 1$). Then the local diffraction field near an isolated zero can be written in the form

$$\psi(\boldsymbol{r}; k) = \boldsymbol{a} \cdot (\boldsymbol{r} - (k-1)\boldsymbol{s}), \tag{2}$$

where $\boldsymbol{a}$ is a complex vector, describing the elliptic anisotropy of the core of the singularity (Schechner and Shamir 1996, Berry and Dennis 2001), and $\boldsymbol{s}$ is a real vector. This can be expressed in the simplest form by choosing the x direction to lie along $\boldsymbol{s}$ and then introducing the scaled coordinates X, Y by

$$x \equiv |\boldsymbol{s}|\left(X - \frac{\mathrm{Re}(a_y/a_x)}{\mathrm{Im}(a_y/a_x)}Y\right), \qquad y \equiv \frac{|\boldsymbol{s}|}{\mathrm{Im}(a_y/a_x)}Y. \tag{3}$$

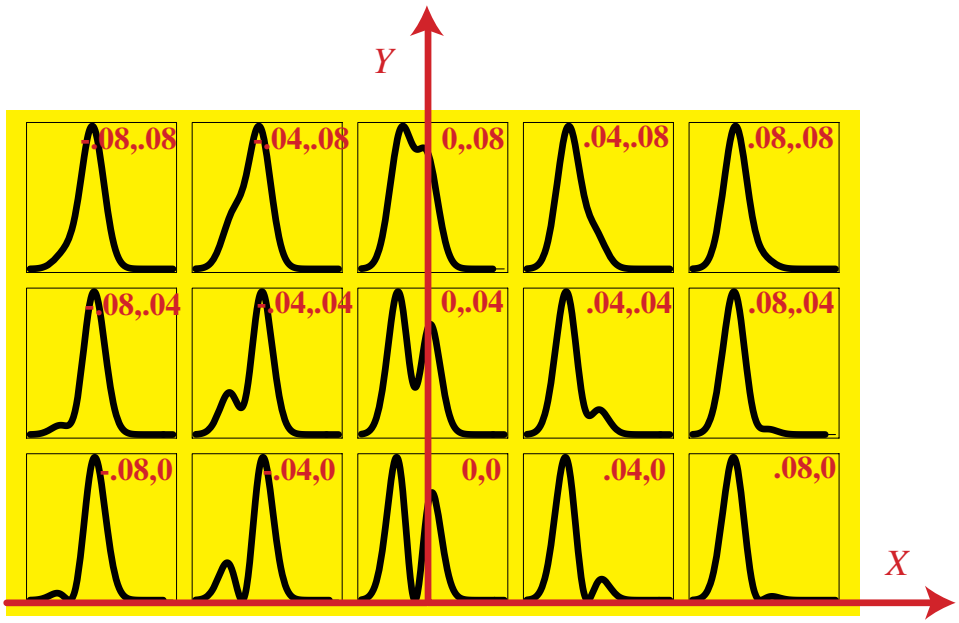

Figure 1. I_{yellow} (equation (6)) near the phase singularity, for k in the visible range $0.7 < k < 1.5$ (vertical scales are arbitrary).

A short calculation brings ψ to the standard form

$$\psi(\boldsymbol{r}; k) = a_x|\boldsymbol{s}|(X - k + 1 + \mathrm{i}Y), \tag{4}$$

so the intensity spectrum of the light at X, Y is, up to an unimportant constant factor,

$$I(k; X, Y) = S_0(k)[(X - k + 1)^2 + Y^2]. \tag{5}$$

The expansion (2) contains the lowest-order terms in $\boldsymbol{r}$ and $k - 1$, which is sufficient to calculate the colours near the singularity in the generic case being studied here. Of course higher-order terms exist too. For example, the vector $\boldsymbol{a}$ in (2) is almost always k-dependent (because on the average singularities are separated by a wavelength so $|\boldsymbol{a}|$ is, on the average, of order k). Such higher-order terms would be necessary to describe colours farther from the singularity, or in nongeneric cases such as $\boldsymbol{s} = 0$ (i.e. the position of the singularity is independent of k) or a_y/a_x real. Many nongeneric situations, arising in experimental situations with particular symmetries, or where singularities coalesce, can be envisaged. Their systematic study would be a useful extension of the generic case considered in the present paper.

The expression (5) describes the spectrum at different points near any typical isolated phase singularity, up to the linear distortions (rotation, shear and dilation) described by (3). For a source spectrum $S_0(k)$ with a single maximum (as for example black-body radiation), the intensity (5) has a now well-understood structure (Gbur *et al* 2002a): two maxima at the origin $X = Y = 0$, that are roughly symmetrical if the maximum of $S_0(k)$ is close to k_Y, as well as the obvious minimum at k_Y. For $Y = 0$ the maxima get more asymmetrical as $|X|$ increases, while for $X = 0$ the central minimum gets shallower as $|Y|$ increases, and eventually disappears. Figure 1 shows an alternative representation of these spectra, that will be explained later. Far from the origin, the spectrum is the same as that of the source, appearing as asymptotic whiteness as will now be described.

3. Tristimulus values and chromaticities near the singularity

An intensity spectrum (e.g. (4) for the light at a given X, Y) is different from a colour, because specification of a spectrum requires infinitely many numbers ($I(k)$ for each k), while specification of a colour requires three numbers (corresponding to the excitations of the three types of cone in the human retina). Therefore the rendering of a colour also requires three numbers (e.g. the voltages to be applied to the red, green and blue phosphors of a monitor). Alternatively stated, human vision projects the infinite-dimensional space of spectra onto the three-dimensional space of colours.

In the standard CIE (Commission Internationale d'Éclairage) system (Travis 1991, Walker 1996), a colour is specified by three tristimulus values $U_i = \{U, V, W\}$. These are obtained by integrating the spectrum $I(k)$ over the three spectral tristimulus values $\bar{u}_i(\lambda) = \{\bar{u}(\lambda), \bar{v}(\lambda), \bar{w}(\lambda)\}$, describing the spectral responses of the three types of cone in the eye of a standard observer, and tabulated (e.g. by Kaye and Laby 1973) at 81 wavelengths over the range 380 nm $< \lambda <$ 780 nm. In particular, the tristimulus value V represents the luminosity. Figure 1 shows the spectral response near the phase singularity of the 'yellow' cone, that is (cf (5))

$$I_{yellow}(k; X, Y) = \frac{\bar{v}(\lambda_Y/k)}{k^2}((X - k + 1)^2 + Y^2), \tag{6}$$

where the factor $1/k^2$ comes from the transformation from λ to k.

According to the procedure described above, the tristimulus values at each point X, Y are (cf (1))

$$U_i(X, Y) = \int \frac{\mathrm{d}k}{k^2} I(k; X, Y) u_i\left(\frac{\lambda_Y}{k}\right), \tag{7}$$

where the integration is over the visible range. The three numbers $\{U, V, W\}$ completely specify the colour. However, it is also convenient to specify colour without regard to intensity. This requires only two numbers; in the conventional (CIE) normalization, these are the chromaticity coordinates (hereinafter called chromaticities), defined by

$$\xi \equiv \frac{U}{X + Y + Z}, \qquad \eta \equiv \frac{V}{X + Y + Z}. \tag{8}$$

Figure 2 shows the colours (rendered as explained in the next section) in the ξ, η space of chromaticities. All colours are contained within the curved locus of pure spectral (i.e. fully saturated) colours (obtained by replacing U, V, W in (8) by $\bar{u}(\lambda), \bar{v}(\lambda), \bar{w}(\lambda)$ and varying λ through the visible range), and the line of purples joining the red and blue ends of the spectral locus.

It is common to evaluate the integrals in (6) as sums, using the tabulated $\bar{u}_i(\lambda)$. However, more insight can be obtained by evaluating the tristimulus values and chromaticities analytically, using the fact that the products of the spectral tristimulus values with the source spectrum S_0 can be fitted accurately by Gaussian functions of k for the cases of principal interest. The fits (reflecting the fact that $\bar{u}(\lambda)$ has two maxima, while $\bar{v}(\lambda)$ and $\bar{w}(\lambda)$ each have one maximum) are

$$\begin{aligned}
\frac{S_0(k)}{k^2}\bar{u}(\lambda) &\approx a_{u1}\exp(-(k - k_{u1})^2/2s_{u1}^2) + a_{u2}\exp(-(k - k_{u2})^2/2s_{u2}^2) \\
\frac{S_0(k)}{k^2}\bar{v}(\lambda) &\approx a_v \exp(-(k - k_v)^2/2s_v^2) \\
\frac{S_0(k)}{k^2}\bar{w}(\lambda) &\approx a_w \exp(-(k - k_w)^2/2s_w^2).
\end{aligned} \tag{9}$$

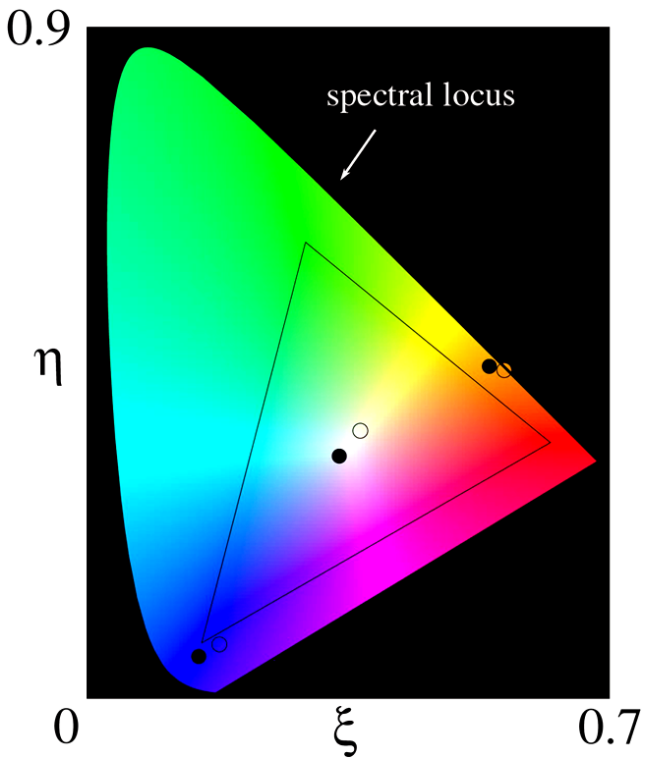

Figure 2. Colours (rendered as explained in section 4) in the plane of chromaticities ξ, η. Filled circles indicate the colours of asymptotic white (centre), and the two 'eyes' (left and right) for a flat spectrum; open circles indicate the corresponding colours for black-body illumination with 4500 K. the triangle indicates the colour gamut of a generic RGB monitor.

Table 1 shows the coefficients in these formulae for several sources of interest, and figure 3 shows the corresponding fits.

The form of (5) implies that the tristimulus values (7) are constant on circles in the X, Y plane, and (9) gives the explicit expressions (ignoring an irrelevant factor $\sqrt{(2\pi)}$)

$$\begin{aligned} U(X,Y) &= a_{u1}s_{u1}((X-k_{u1}+1)^2+Y^2+s_{u1}^2)+a_{u2}s_{u2}((X-k_{u2}+1)^2+Y^2+s_{u2}^2) \\ V(X,Y) &= a_v s_v((X-k_v+1)^2+Y^2+s_v^2) \\ W(X,Y) &= a_w s_w((X-k_w+1)^2+Y^2+s_w^2). \end{aligned} \tag{10}$$

Note that the luminosity V is never zero, but has a finite minimum at $X = k_v$, for the obvious reason that the phase singularities for different k are in different places.

From (8) and (10), the chromaticities are

$$\begin{aligned} \xi &= \xi_{white}\frac{X^2+Y^2+2aX+\alpha}{X^2+Y^2+2tX+\tau}, \\ \eta &= \eta_{white}\frac{X^2+Y^2+2bX+\beta}{X^2+Y^2+2tX+\tau}. \end{aligned} \tag{11}$$

Table 1. Coefficients in (9) for four sources.

Spectrum S_0	Flat ($S_0 = 1$)	3300 K	4500 K	6000 K
a_{u1}	1.25	1.48	1.25	1.16
a_{u2}	0.239	0.105	0.175	0.231
a_v	1.02	1.04	1.02	0.994
a_w	1.17	0.555	0.865	1.20
k_{u1}	0.94	0.924	0.93	0.993
k_{u2}	1.25	1.22	1.25	1.26
k_v	0.993	0.977	0.99	1.00
k_w	1.24	1.22	1.23	1.23
s_{u1}	0.05	0.05	0.05	0.05
s_{u2}	0.05	0.06	0.06	0.06
s_v	0.07	0.07	0.07	0.07
s_w	0.065	0.065	0.065	0.065

Here ξ_{white} and η_{white} are the chromaticities of the 'asymptotic white' far from the singularity, given by

$$\begin{aligned} \xi_{white} &= \frac{a_{u1}s_{u1} + a_{u2}s_{u2}}{a_{u1}s_{u1} + a_{u2}s_{u2} + a_v s_v + a_w s_w}, \\ \eta_{white} &= \frac{a_v s_v}{a_{u1}s_{u1} + a_{u2}s_{u2} + a_v s_v + a_w s_w}, \end{aligned} \tag{12}$$

and

$$\begin{aligned} a &= \frac{(1-k_{u1})a_{u1}s_{u1} + (1-k_{u2})a_{u2}s_{u2}}{a_{u1}s_{u1} + a_{u2}s_{u2}} \\ \alpha &= \frac{((1-k_{u1})^2 + s_{u1}^2)a_{u1}s_{u1} + ((1-k_{u2})^2 + s_{u2}^2)a_{u2}s_{u2}}{a_{u1}s_{u1} + a_{u2}s_{u2}} \\ b &= 1 - k_v, \quad \beta = (1-k_v)^2 + s_v^2 \\ t &= \frac{(1-k_{u1})a_{u1}s_{u1} + (1-k_{u2})a_{u2}s_{u2} + (1-k_v)a_v s_v + (1-kw)a_w s_w}{a_{u1}s_{u1} + a_{u2}s_{u2} + a_v s_v + a_w s_w} \\ \tau &= \frac{\left(\begin{array}{c} ((1-k_{u1})^2 + s_{u1}^2)a_{u1}s_{u1} + ((1-k_{u2})^2 + s_{u2}^2)a_{u2}s_{u2} \\ + ((1-k_v)^2 + s_v^2)a_v s_v + ((1-k_w)^2 + s_w^2)a_w s_w \end{array} \right)}{a_{u1}s_{u1} + a_{u2}s_{u2} + a_v s_v + a_w s_w}. \end{aligned} \tag{13}$$

The expressions (11) reveal much about the colours near the singularity. Contours of constant value of each of the chromaticities $\xi(X, Y)$ and $\eta(X, Y)$ (figures 4(a), (b)) consist of two families of non-concentric circles, centred at points on the X axis, separated by a line parallel to the Y axis. If one of the ξ-circles were to coincide with one of the η-circles, this would be a circle of constant colour in the XY plane, but this cannot happen (appendix). However, it almost happens, in the sense that the patterns of ξ- and η-circles nearly overlap (figure 4(c)).

This means that the pattern is built from two sets of approximately isocoloured circles in the XY plane, whose principal features are two coloured 'eyes' (zero-radius circles); far from

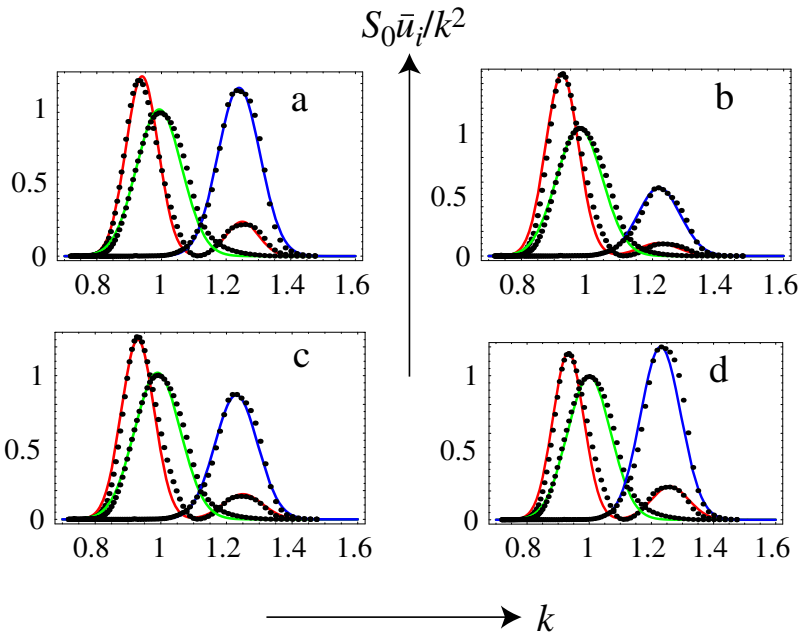

Figure 3. Gaussian fits (9) of tristimulus values (red: $\bar{u}$; green: $\bar{v}$; blue: $\bar{w}$) compared with the corresponding quantities evaluated from the tabulated values (Kaye and Laby 1973) (dotted curves), for: (a) source with a flat spectrum; (b) black-body source, $T = 3300$ K; (c) black-body source, $T = 4500$ K; (d) black-body source, $T = 6000$ K. The small discrepancies hardly affect subsequent colour renderings.

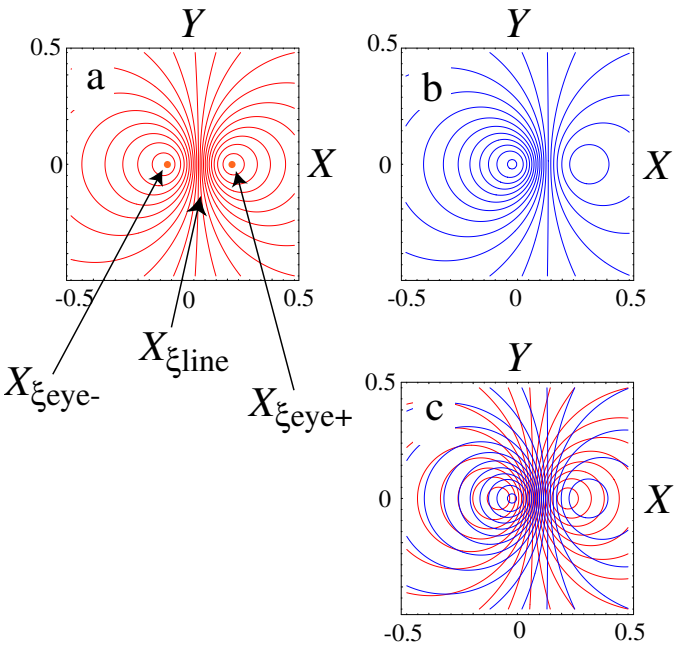

Figure 4. Chromaticity contours for a flat source spectrum; (a): ξ-circles; (b): η-circles; (c): superposition of (a) and (b).

Table 2. Chromaticities of significant features of pattern near a phase singularity, for four sources.

Source	Flat	3300 K	4500 K	6000 K
ξ_{white}	0.336	0.424	0.364	0.327
η_{white}	0.322	0.385	0.356	0.317
ξ_{eye+}	0.538	0.587	0.558	0.554
η_{eye+}	0.443	0.420	0.438	0.430
ξ_{eye-}	0.146	0.161	0.174	0.172
η_{eye-}	0.052	0.102	0.068	0.053

the 'eyes', the pattern at infinity is the asymptotic white already discussed. Calculations based on (11) (appendix) show that the colours of the 'eyes' are

$$\begin{aligned}\frac{\xi_{eye\pm}}{\xi_{white}} &= \frac{\alpha+\tau-2ta \pm \sqrt{(\alpha+\tau-2ta)^2-4(t^2-\tau)(a^2-\alpha)}}{2(\tau-t^2)},\\ \frac{\eta_{eye\pm}}{\eta_{white}} &= \frac{\beta+\tau-2tb \pm \sqrt{(\beta+\tau-2tb)^2-4(t^2-\tau)(b^2-\beta)}}{2(\tau-t^2)}.\end{aligned} \tag{14}$$

Table 2 shows the chromaticites for the asymptotic white and for the 'eyes', for several different sources. The straight line contours reaching out to the asymptotic whiteness are $X_{\xi\,line}$ and $X_{\eta\,line}$, given (as is obvious from (11)), by

$$X_{\xi\,line} = \frac{\alpha-\tau}{2(t-a)}, \qquad X_{\eta\,line} = \frac{\beta-\tau}{2(t-b)}. \tag{15}$$

The positions of the 'eyes' are

$$X_{\xi\,eye\pm} = X_{\xi\,line} \pm D_\xi, \qquad X_{\eta\,eye\pm} = X_{\eta\,line} \pm D_\eta, \qquad Y = 0, \tag{16}$$

where

$$\begin{aligned}D_\xi &= \frac{\sqrt{(\alpha-\tau)^2+4(a-t)(a\tau-\alpha t)}}{2(t-a)},\\ D_\eta &= \frac{\sqrt{(\beta-\tau)^2+4(b-t)(b\tau-\beta t)}}{2(t-b)}.\end{aligned} \tag{17}$$

Table 3 shows these approximate positions, for the lines and for the eyes, for several different sources, and the colours of the eyes and the asymptotic white are shown for two sources in figure 2.

Of the approximately isocoloured circles surrounding the 'eyes' in the XY plane, the most prominent will be that corresponding to the brightest white that the rendering device can display ('monitor white'). Obviously this colour is independent of the source spectrum. This white circle lies between the two circular contours obtained by setting ξ and η in (11) to their monitor-white values. Figure 5 shows the two circles, in the XY plane, within which the bright white circle lies, and the two points between which the intensely-coloured 'eyes' lie, for four different sources.

Note that the various features in figure 2 lie in the lower half of the chromaticity diagram. In fact all the colours near a phase singularity lie in a rather small region, contrary to the initial

Table 3. Approximate locations of significant features of colour pattern near a phase singularity.

Source	Flat	3300 K	4500 K	6000 K
$X_{\xi\,line}$	0.072	0.042	0.051	0.430
$X_{\eta\,line}$	0.138	0.173	0.149	0.145
$X_{\xi\,eye+}$	0.221	0.177	0.195	0.202
$X_{\eta\,eye+}$	0.299	0.381	0.323	0.306
$X_{\xi\,eye-}$	−0.077	−0.092	−0.094	−0.098
$X_{\eta\,eye-}$	−0.023	−0.035	−0.025	−0.016

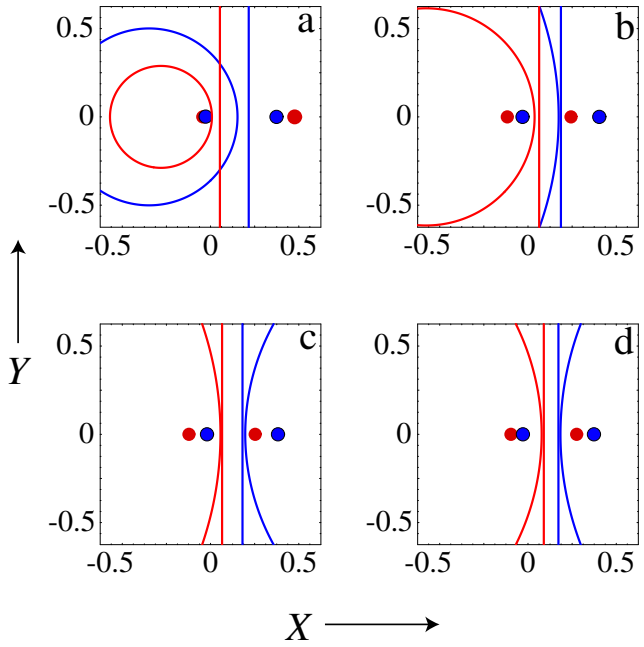

Figure 5. Chromaticity contours of ξ (red) and η (blue) for (a): black-body source, $T = 3300$ K; (b): black-body source, $T = 4500$ K; (c): black-body source, $T = 6000$ K; (d): flat spectrum; the large circles are the contours for monitor white ($\xi = 0.31, \eta = 0.33$), the straight lines are contours for asymptotic white (table 2), and the dots represent the intensely-coloured 'eyes'.

expectation that every colour will appear somewhere. To establish this surprising result, it is helpful to regard (11) as a map from the diffraction plane XY to the chromaticity plane $\xi\eta$. The region of explored colours lies within the locus of singularities of this map, where the Jacobian determinant of the equations (11) vanishes. Calculation shows that the determinant vanishes when $Y = 0$, so the locus is given parametrically by varying X in (11) with $Y = 0$. The locus is an ellipse, shown in figure 6 for flat illumination, though the picture is similar for all white light sources.

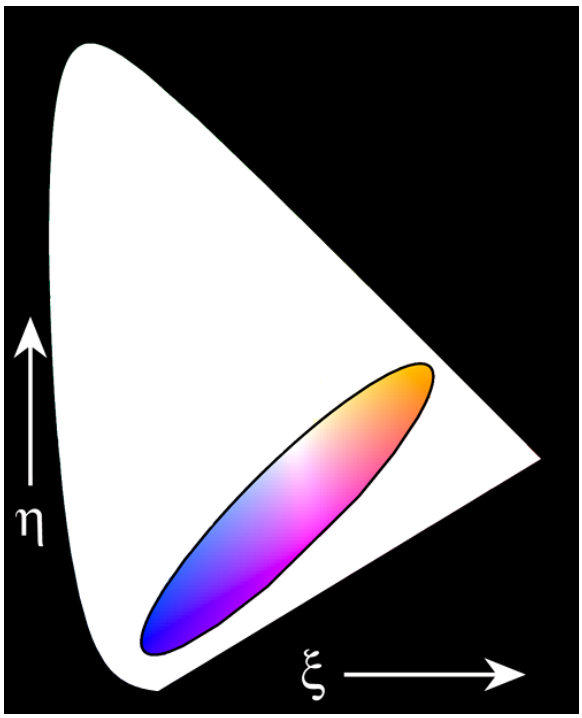

Figure 6. Domain of chromaticity space explored near an isolated phase singularity, for a flat source spectrum. The elliptical region is similarly situated for black-body sources of visible light. Note the absence of green.

The limited range of colours is remarkable, but not unprecedented: the fraction of possible colours in the natural rainbow is similarly surprisingly small (Lee 1991, Lee and Fraser 2001)—though rainbow colours are very different from the 'dark colours' we are studying here. A particular feature of the present pattern is that there is no green. This can be explained in elementary terms by the observation that the spectrum is shifted towards the blue on one side of the singularity, and towards the red on the other side, with the roughly symmetrical mixture of red and blue between, above and below being strongly desaturated and so giving white rather than green. The absence of green near a coloured phase singularity contrasts sharply with the asymptotic alternation of green and pink that characterises two-wave interference fringes in white light (Berry and Wilson 1994, Berry and Klein 1996).

4. Rendering the colours

The next step is to simulate the predicted colours on a monitor screen, by calculating from the tristimulus values $U_i(X,Y)$ (equation (10)) the R, G, B values to employ in a colour-rendering program. Colour rendering that is reproducible across different monitors and printers is notoriously tricky; the intellectual centre of the problem lies somewhere inside the triangle whose vertices are science, art and craft. Here I adhere to current best practice (Travis 1991, Walker 1996, Hamilton 1999, 2001), but caution that the colours to be reproduced are at best guides to what to expect in an experiment. The rendering procedure is based on four stages,

expressed symbolically as

$$\begin{pmatrix} R \\ G \\ B \end{pmatrix} \underset{(a)}{=} \mathbf{M}^{-1} \begin{pmatrix} U \\ V \\ W \end{pmatrix} \underset{(b)}{\Rightarrow} \begin{pmatrix} R \\ G \\ B \end{pmatrix} - \min(R, G, B, 0) \begin{pmatrix} 1 \\ 1 \\ 1 \end{pmatrix}$$
$$\underset{(c)}{\Rightarrow} \begin{pmatrix} R \\ G \\ B \end{pmatrix}^{1/\gamma} \underset{(d)}{\Rightarrow} \begin{pmatrix} R \\ G \\ B \end{pmatrix} \Big/ \max(R, G, B), \tag{18}$$

and which will now be explained.

In stage (a), the matrix $\mathbf{M}$ is constructed from the chromaticities ξ, η of the red, green and blue phosphors of the monitor being employed:

$$\mathbf{M} = \begin{pmatrix} \xi_R & \xi_G & \xi_B \\ \eta_R & \eta_G & \eta_B \\ 1 - \xi_R - \eta_R & 1 - \xi_G - \eta_G & 1 - \xi_B - \eta_B \end{pmatrix}. \tag{19}$$

In what follows, I used the 'generic RGB monitor' values

$$\xi_R = 0.64, \eta_R = 0.33; \qquad \xi_G = 0.30, \eta_G = 0.60; \qquad \xi_B = 0.15, \eta_B = 0.06, \tag{20}$$

and the corresponding monitor white $\xi = 0.31$, $\eta = 0.33$.

Stage (b) compensates for the fact that some of the colours being rendered lie outside the gamut of the monitor screen, as indicated by one or more of the R, G, B values from stage (a) being negative. The particular compensation employed here (Hamilton 1999) desaturates the R, G, B values by adding just enough monitor white to bring the colour to the triangular boundary of the screen's gamut (figure 2); however, alternative compensations (e.g. replacing each negative R, G, B value by zero) lead to similar-looking renderings. This compensation is an unavoidable limitation of computer screens (and colour printing) and means that in figure 2, and the renderings to follow in figure 7, all colours outside the gamut are imperfectly rendered. In particular this applies to the highly saturated colours of the 'eyes' near a phase singularity.

Stage (c) is the 'gamma correction' compensating for the nonlinearity of the screen (brightness not proportional to R, G, B); I chose the typical value $\gamma = 1.8$.

Stage (d) standardizes the brightness across the simulation, by setting the biggest R, G, B value at each point equal to unity. In the present application this is particularly important, because near the phase singularity the light intensity is very small (though of course not zero as for monochromatic illumination); without this final compensation, all the predicted colours would be lost in darkness.

Figure 7 shows some sample renderings, calculated for several different sources. Figure 8 is a three-dimensional representation of the colours, showing the luminosity falling to a parabolic minimum in the region of the singularity. The following points should be noted:

(i) All the pictures look rather similar, except for the obvious yellowing as the colour temperature of the source decreases.

(ii) Far from the singularity, the image is white, with the asymptotic whiteness being yellower for cooler sources.

(iii) The left and right 'eyes' show the intense blue and orange, separated by red, expected from the theoretical analysis.

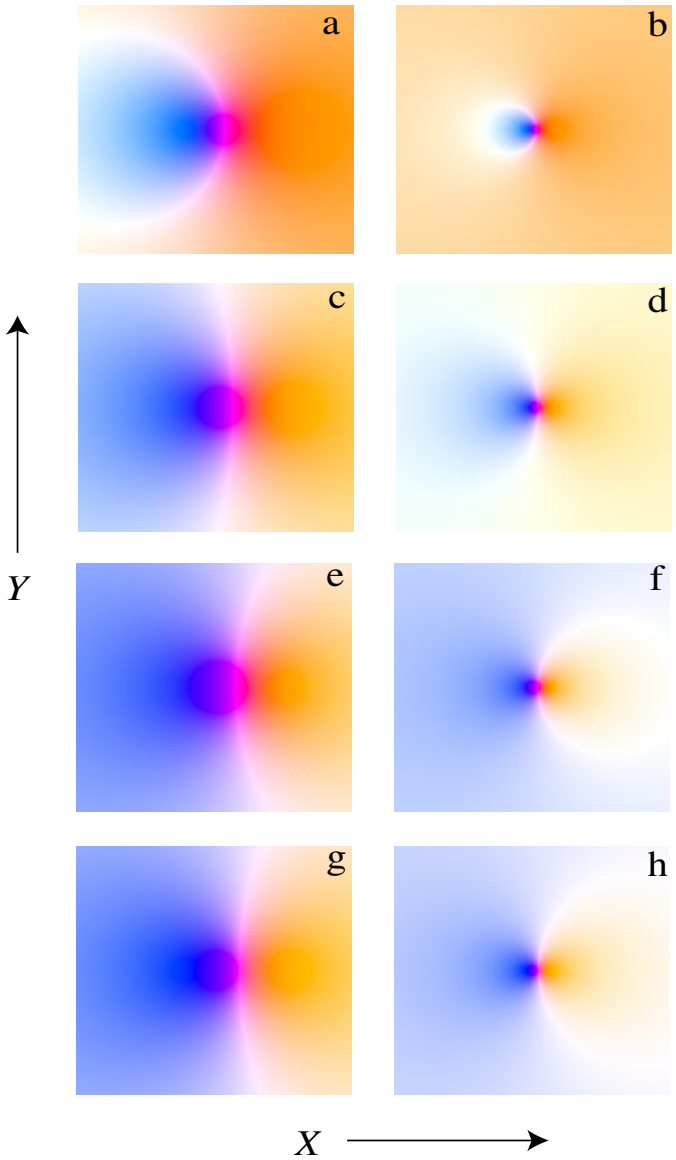

Figure 7. Simulations of colours near a phase singularity, for the following sources: (a), (b), black-body, $T = 3300$ K; (c), (d), black-body, $T = 4500$ K; (e), (f), black-body, $T = 6000$ K; (g), (h), flat. In (a), (c), (e), (g), the range is $(|X, Y|) < 0.5$; in (b), (d), (f), (h), the range is $(|X, Y|) < 1$.

(iv) The prominent white circle surrounds the blue eye for cooler sources, and the orange eye for hotter sources, the boundary between these cases corresponding to a colour temperature of about 5500 K, for which the asymptotic white corresponds to the monitor white; in each case the white circle lies, as predicted, between the ξ and η contours in figure 5, corresponding to monitor white.

(v) Green is absent.

(vi) As mentioned previously, all colours are approximate.

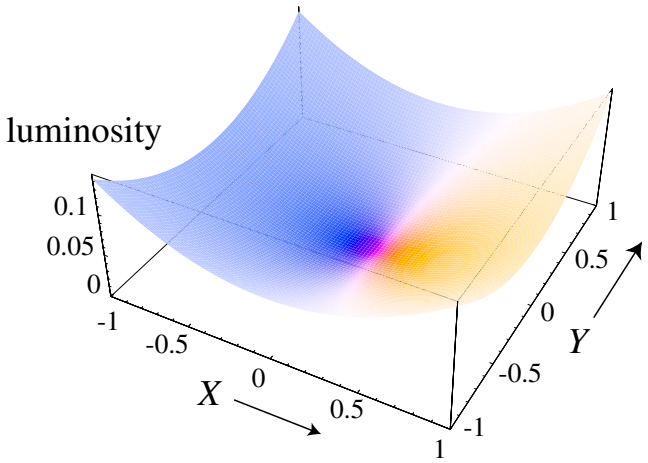

Figure 8. Luminosity $V(X, Y)$ near a phase singularity, coloured according to chromaticities, for a flat spectrum.

5. Proposed experiment

The colour pattern resulting from the foregoing analysis of the appearance of the simplest diffraction phenomenon—an isolated zero in white light—is unexpectedly rich and subtle, and it is desirable to test the various predictions by experiment. The following observations should be incorporated into the design of any experiment.

(i) The theory is intended to apply to a phase singularity 'in the wild', where the position of the zero is colour dependent. Therefore a too-symmetrical setup, where the singularity is in the same place for all wavelengths (i.e. $\boldsymbol{s} = 0$ in equation (2)), must be avoided (see the remarks following equation (5)).

(ii) The chosen phase singularity should be isolated, in the sense explained in section 2.

(iii) Any broadband source of white light (e.g. a tungsten or a halogen lamp) should work.

(iv) The neighbourhood of a phase singularity is dark, and in order to see the predicted colours it is essential to scale the observations to constant luminosity. This is possible because in the situation envisaged here the intensity never falls to zero, but rather to a parabolic minimum.

(v) The observed pattern is likely to be a linearly distorted version of the 'universal' images of figure 7, so the data should be 'rectified' to compensate this.

Appendix. Algebra of colour circles

The chromaticity formulae (11) can be written in the transparent form

$$(X - X_\xi)^2 + Y^2 = R_\xi^2, \qquad (X - X_\eta)^2 + Y^2 = R_\eta^2, \tag{A.1}$$

where, denoting ξ/ξ_{white} by ξ', and η/η_{white} by η',

$$\begin{aligned} X_\xi &= \frac{t\xi' - a}{1 - \xi'}, \qquad & R_\xi^2 &= \frac{\tau\xi' - \alpha}{1 - \xi'} + X_\xi^2, \\ X_\eta &= \frac{t\eta' - b}{1 - \eta'}, \qquad & R_\eta^2 &= \frac{\tau\eta' - \beta}{1 - \eta'} + X_\eta^2. \end{aligned} \tag{A.2}$$

Thus the contours for chromaticities ξ and η are circles with radii R_ξ and R_η, centred on X_ξ and X_η.

For a pair of these circles to coincide, the chromaticity must satisfy

$$\xi' = \frac{\eta'(t-a)+a-b}{t-b}, \qquad \xi' = \frac{\eta'(\tau-\alpha)+\alpha-\beta}{\tau-\beta}. \tag{A.3}$$

Equating these values of ξ', and using the identity

$$(\tau-\alpha)(t-b)-(t-a)(\tau-\beta) = (a-b)(\tau-\beta)-(a-\beta)(t-b), \tag{A.4}$$

implies that the only solution of the coincidence equation (A.3) is the trivial $\xi = \xi_{white}, \eta = \eta_{white}$, corresponding (cf (A.2)) to infinitely large circles centred at infinity on the X axis. These lines, with intersections of the X axis at two different places, are given by (15). This completes the proof that the ξ-circles and the η-circles cannot coincide.

The ξ-eyes correspond to $R_\xi = 0$, and the η-eyes correspond to $R_\eta = 0$. Use of (A.2) now reproduces (14). The positions of the eyes (equations (16) and (17)), now follow from equation (A.2) after using (14).

References

Berry M V and Dennis M R 2001 Polarization singularities in isotropic random waves *Proc. R. Soc.* A **457** 141–55

Berry M V and Klein S 1996 Colored diffraction catastrophes *Proc. Natl Acad. Sci. USA* **93** 2614–19

Berry M V and Wilson A N 1994 Black-and-white fringes and the colours of caustics *Appl. Opt.* **33** 4714–18

Foley J T and Wolf E 2002 The phenomenon of spectral switches as a new effect in singular optics with polychromatic light *J. Opt. Soc. Am.* A submitted

Gbur G, Visser T D and Wolf E 2002a Anomalous behavior of spectra near phase singularities of focused waves *Phys. Rev. Lett.* **88** 013901

Gbur G, Visser T D and Wolf E 2002b Singular behavior of the spectrum in the neighborhood of focus *J. Opt. Soc. Am.* A submitted

Hamilton A J S H 1999 Where's purple? Or, how to plot colours properly on a computer screen http://casa.colorado.edu/∼ajsh/colour/rainbow.html#eq3

Hamilton A J S H 2001 What colour is the Sun? http://casa.colorado.edu/∼ajsh/colour/Tspectrum.html

Kaye G W C and Laby T H 1973 *Tables of Physical and Chemical Constants* (London: Longman)

Lee R L 1991 What are 'all the colors of the rainbow'? *Appl. Opt.* **30** 3401–7

Lee R L and Fraser A 2001 *The Rainbow Bridge: Rainbows in Myth, Art and Science* (Bellingham, WA: SPIE and Pennsylvania State University Press)

Nye J F 1999 *Natural Focusing and Fine Structure of Light: Caustics and Wave Dislocations* (Bristol: Institute of Physics Publishing)

Ponomarenko S A and Wolf E 2002 Spectral anomalies in a Fraunhofer diffraction pattern *Opt. Lett.* submitted

Popescu G and Dogariu A 2002 Spectral anomalies at wavefront dislocations *Phys. Rev. Lett.* **88** 183902

Schechner Y Y and Shamir J 1996 Parameterization and orbital angular momentum of anisotropic dislocations *J. Opt. Soc. Am.* A **13** 967–73

Soskin M S and Vasnetsov M V 2001 Singular optics *Prog. Opt.* **42** 219–76

Travis K T 1991 *Effective Color Displays: Theory and Practice* (London: Academic)

Walker J 1996 Colour rendering of spectra http://www.fourmilab.ch/documents/specrend/